Integral elastic, electronic-state, ionization, and total cross sections for electron scattering with furfural

D. B. Jones, R. F. da Costa, M. T. do N. Varella, M. H. F. Bettega, M. A. P. Lima, F. Blanco, G. García, and M. J. Brunger'

Citation: J. Chem. Phys. **144**, 144303 (2016); doi: 10.1063/1.4945562

View online: http://dx.doi.org/10.1063/1.4945562

View Table of Contents: http://aip.scitation.org/toc/jcp/144/14

Published by the American Institute of Physics

Integral elastic, electronic-state, ionization, and total cross sections for electron scattering with furfural

D. B. Jones,[1] R. F. da Costa,[2,3] M. T. do N. Varella,[4] M. H. F. Bettega,[5] M. A. P. Lima,[2] F. Blanco,[6] G. García,[7] and M. J. Brunger[1,8,a)]

[1]*School of Chemical and Physical Sciences, Flinders University, GPO Box 2100, Adelaide, South Australia 5001, Australia*
[2]*Instituto de Física "Gleb Wataghin," Universidade Estadual de Campinas, Campinas, 13083-859 São Paulo, Brazil*
[3]*Departamento de Física, Universidade Federal do Espírito Santo, 29075-910, Vitória, Espírito Santo, Brazil*
[4]*Instituto de Física, Universidade de São Paulo, CP 66318, 05315-970 São Paulo, Brazil*
[5]*Departamento de Física, Universidade Federal do Paraná, CP 19044, 81531-990 Curitiba, Paraná, Brazil*
[6]*Departamento de Física Atómica, Molecular y Nuclear, Universidad Complutense de Madrid, Madrid E-28040, Spain*
[7]*Instituto de Física Fundamental, CSIC, Serrano 113-bis, 28006 Madrid, Spain*
[8]*Institute of Mathematical Sciences, University of Malaya, 50603 Kuala Lumpur, Malaysia*

(Received 8 March 2016; accepted 24 March 2016; published online 8 April 2016)

We report absolute experimental integral cross sections (ICSs) for electron impact excitation of bands of electronic-states in furfural, for incident electron energies in the range 20–250 eV. Wherever possible, those results are compared to corresponding excitation cross sections in the structurally similar species furan, as previously reported by da Costa *et al*. [Phys. Rev. A **85**, 062706 (2012)] and Regeta and Allan [Phys. Rev. A **91**, 012707 (2015)]. Generally, very good agreement is found. In addition, ICSs calculated with our independent atom model (IAM) with screening corrected additivity rule (SCAR) formalism, extended to account for interference (I) terms that arise due to the multi-centre nature of the scattering problem, are also reported. The sum of those ICSs gives the IAM-SCAR+I total cross section for electron–furfural scattering. Where possible, those calculated IAM-SCAR+I ICS results are compared against corresponding results from the present measurements with an acceptable level of accord being obtained. Similarly, but only for the band I and band II excited electronic states, we also present results from our Schwinger multichannel method with pseudopotentials calculations. Those results are found to be in good qualitative accord with the present experimental ICSs. Finally, with a view to assembling a complete cross section data base for furfural, some binary-encounter-Bethe-level total ionization cross sections for this collision system are presented. © *2016 AIP Publishing LLC.* [http://dx.doi.org/10.1063/1.4945562]

I. INTRODUCTION

We initially became interested in furfural ($C_5H_4O_2$) due to its importance in many industries[1] and, in particular, due to its possible production through atmospheric-plasma treatments of biomass.[2,3] In any likely application of the latter, for example, through the commercial establishment of a bio-refinery, the plasma action will need to be understood through some form of modelling or simulation, with electron scattering cross sections for all relevant species in the plasma being just one of the required inputs. It is hoped that fundamental scattering data of key biomass subunits, and their inclusion in plasma models, can provide insights into the mechanisms of those plasma actions with different forms of biomass that are built from varying fractions of complex polymers (cellulose, hemicellulose, and lignin). As a consequence, we have undertaken a systematic study of electron and photon interactions with furfural, both experimental and theoretical, that probed its valence electronic structure, vibrational quanta, elastic scattering and discrete electronic-state excitation differential cross sections (DCSs) and ionization phenomena.[4–8] The present submission is a new step in this series of investigations with furfural, and as it is the integral cross sections (ICSs) that are generally of most interest to the modelling communities[9–14] it therefore represents an important achievement. Note that this follows on from a similarly extensive study on phenol,[15–20] another important by-product from the application of atmospheric-pressure plasmas to biomass.

While our independent atom model with screening corrected additivity rule (IAM-SCAR) calculations have had some success, in describing the electron scattering process down to energies (E_0) ~ 20 eV with some molecules,[21–23] there are other systems[24–26] where this approach does not yield cross sections that are in agreement with measured data for energies as high as 50 eV. In response to this, at least in part, Blanco and García[27] recently extended their IAM-SCAR approach to account for multi-centre scattering (i.e., interference (I)) effects (thus now known as the IAM-SCAR+I method). We

a)Author to whom correspondence should be addressed. Electronic mail: Michael.Brunger@flinders.edu.au

had previously considered the efficacy of this development, to describing elastic electron scattering from furfural,[8] by comparison to results from a sophisticated Schwinger multichannel (SMC) computation. Here we extend this comparison by investigating how well the IAM-SCAR+I method performs in predicting the inelastic integral cross section sum. Recall that in principle this approach can calculate elastic differential and integral cross sections, inelastic integral cross sections (as a sum of the ICS for discrete inelastic processes, dissociation processes, and ionization) and if the species is polar (as furfural is) rotational ICSs through a Born-dipole method.[21–24] The total cross section is then simply determined as the sum of all the aforementioned ICSs. Testing the validity of the inelastic ICSs from the current IAM-SCAR+I calculations forms a second rationale for the present study.

We have previously noted that furfural and furan are structurally similar molecules.[6,7] This structural similarity also produces comparable features in their ground and excited state electronic structures (extensive discussion of the electronic structures of furan and furfural is available[4,5,28–30]), so that a comparison between their complementary cross sections might be feasible. In this case, the band I electronic-states in furfural[4,7] might correspond to the excitation of the $^3B_2$ electronic-state in furan.[31,32] That excitation is a (HOMO) → (LUMO) process, which is similar to the excitation of the $^3A'$ electronic-state (in band I) in furfural.[4] Specifically, the HOMOs of both species are dominated by the out-of-plane π-bonding of the furan ring and the LUMOs correspond to the π^*-furan ring contribution. Additionally excitation of the $^3A_1$ state in furan is a (HOMO − 1) → (LUMO) process[31,32] that corresponds to excitation of the $^3A'$ state (in band II) in furfural.[4] This transition is characterised by an excitation from the out-of-plane O(2*p*)/C(2*p*) ring *p*-bonding network to the π^*-furan ring orbital. Lastly, excitation of the $^1B_2$ electronic-state of furan is a (HOMO) → (LUMO) process that is similar to that for the $^1A'$ state (in band II) in furfural, the singlet version of the $\pi\pi^*$ transition in band I. The significant localisation of the contributing orbitals to the ring suggests that, to first order, the $^3B_2$ ICS of da Costa *et al.*[31] and Regeta and Allan[32] in furan can be compared to the present ICSs for band I in furfural, while the furan ($^3A_1$ + $^1B_2$) integral cross sections of Regeta and Allan[32] can be compared to the present ICSs for band II in furfural. This comparison forms another rationale for our current investigation.

The structure of the remainder of this paper is as follows. In Sec. II, we briefly describe our procedure for deriving the absolute ICSs from our DCS measurements,[4,7] as well as presenting a précis of our IAM-SCAR+I and Schwinger multichannel method with pseudopotentials (SMCPP) computations. Thereafter, in Sec. III, our measured furfural ICS results for bands I–IV, our theoretical results (binary-encounter-Bethe (BEB),[33] SMCPP,[7] and IAM-SCAR+I[27]) and a comparison, where possible, between them will be presented and discussed. In addition, a comparison between the relevant furfural and furan electronic-state ICSs will also be provided in this section. Finally, some conclusions arising from the current investigation are given in Sec. IV.

II. ANALYSIS PROCEDURES AND THEORY

All details pertaining to the excited electronic-state spectroscopy of furfural can be found in the work of Ferreira da Silva *et al.*,[4] and so we do not repeat them here. Rather, we simply note that integral cross sections for the (i) band I excited electronic-states, (ii) band II excited electronic-states, (iii) band III excited electronic-states, (iv) band IV excited electronic-states, (v) band V excited electronic-states, and (vi) band VI excited electronic-states are reported in this paper. The sum of the ICS for those six "discrete" electronic bands are also reported. The energy range for the present ICSs is 20–250 eV, with a listing of those data being given in Table I and plotted in Figs. 1 and 2.

A full discussion of our experimental and data analysis methodologies, in going from measured electron energy loss spectra to deriving the absolute inelastic differential cross sections (DCSs), can be found in the work of Jones *et al.*[7] (to whom the reader is referred for more details). The DCS (σ_i) for a given scattering process, i (in this case i = (i)–(vi) above), is related to the ICS, Q_i, through the standard formula

$$Q_i(E_0) = 2\pi \int_0^\pi \sigma_i(E_0, \theta) \sin\theta d\theta, \tag{1}$$

where E_0 = incident electron energy and θ = scattered electron angle. In order to convert experimental DCS data, measured at discrete angles that span a finite angular range determined by the physical constraints of the apparatus,[34] to an ICS, one must first extrapolate and interpolate the measured data so that they cover the full angular range from 0° to 180°. Our approach to accomplish this, built around a generalised

TABLE I. Present experimental integral cross sections ($\times 10^{-16}$ cm^2) for electron impact excitation of the discrete inelastic bands I–VI in furfural, and their sum. The percentage uncertainties (%) on these derived values are also presented. See text for more details. Note that E_L = energy loss.

	ICS ($\times 10^{-16}$ cm^2)						
E_L (eV)	Band I ~2.7–4.3	Band II ~4.3–5.3	Band III ~5.3–6.4	Band IV ~6.4–7.4	Band V ~7.4–8.2	Band VI ~8.2–9.0	Sum
E_0 (eV)							
20	0.116 (57%)	1.040 (49%)	0.348 (54%)	0.416 (56%)	0.283 (59%)	0.267 (60%)	2.47 (26%)
30	0.063 (61%)	0.801 (45%)	0.280 (46%)	0.490 (46%)	0.467 (46%)	0.547 (46%)	2.65 (21%)
40	0.047 (69%)	0.785 (43%)	0.249 (46%)	0.436 (44%)	0.431 (43%)	0.484 (43%)	2.43 (20%)
250		Bands I+II+III 0.81(25%)			Bands IV+V+VI 1.6 (23%)		2.41 (18%)

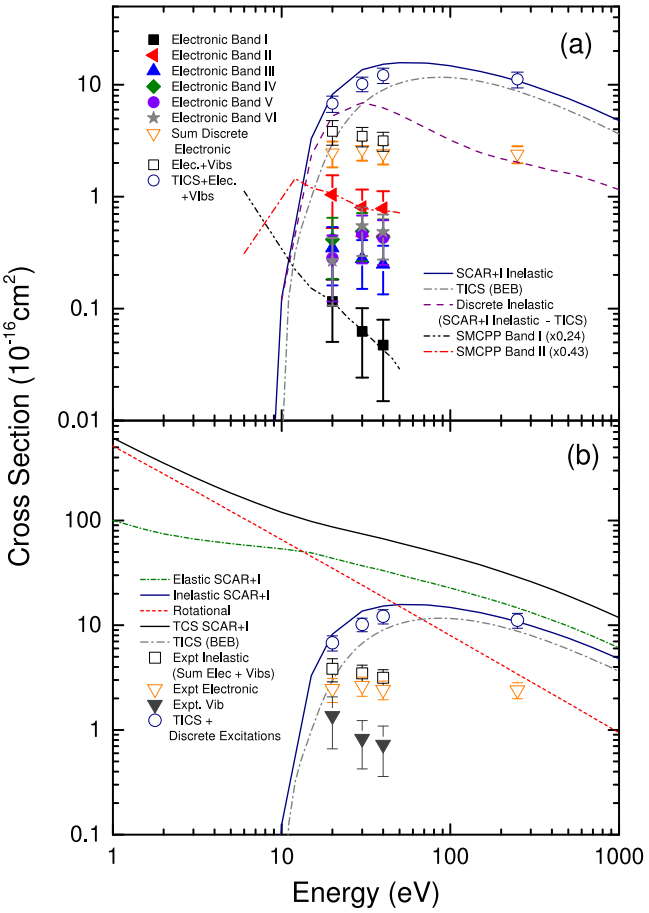

FIG. 1. (a) Integral cross sections ($\times 10^{-16}$ cm^2) for electron impact excitation of the discrete electronic bands I–VI in furfural. Band I denoted by (■), band II denoted by (◄), band III denoted by (▲), band IV denoted by (◆), band V denoted by (●), and band VI denoted by (★). Also shown is the sum of the ICS for those bands (▽), the sum of the electronic ICS and vibrational excitation ICS from work of Jones *et al.* (□),[6] which sum plus a total ionization cross section (TICS) using a BEB calculation[33] (○) and the IAM-SCAR+I ICS for the sum of all open inelastic channels (except vibrational excitation). Finally, our SMCPP results for Bands I and II, scaled by the appropriate factor in each case to give best agreement with the measurements, are also shown. See legend in figure and text for details. (b) Theoretical IAM-SCAR+I ICS results ($\times 10^{-16}$ cm^2) for elastic scattering (green - · - · -), total inelastic scattering (purple —) and the total cross section (TCS) (thin black —) in furfural. Also shown are a rotational ICS using a Born-dipole approach[21–26] (red - - - -), and a total ionization cross section from a BEB calculation (grey – · –).[33] The sum of the available measured electronic-state ICSs (this work), vibrational ICSs,[6] and their sum is also shown, as is the TICS + discrete excitations sum. See legend in figure and text for further details.

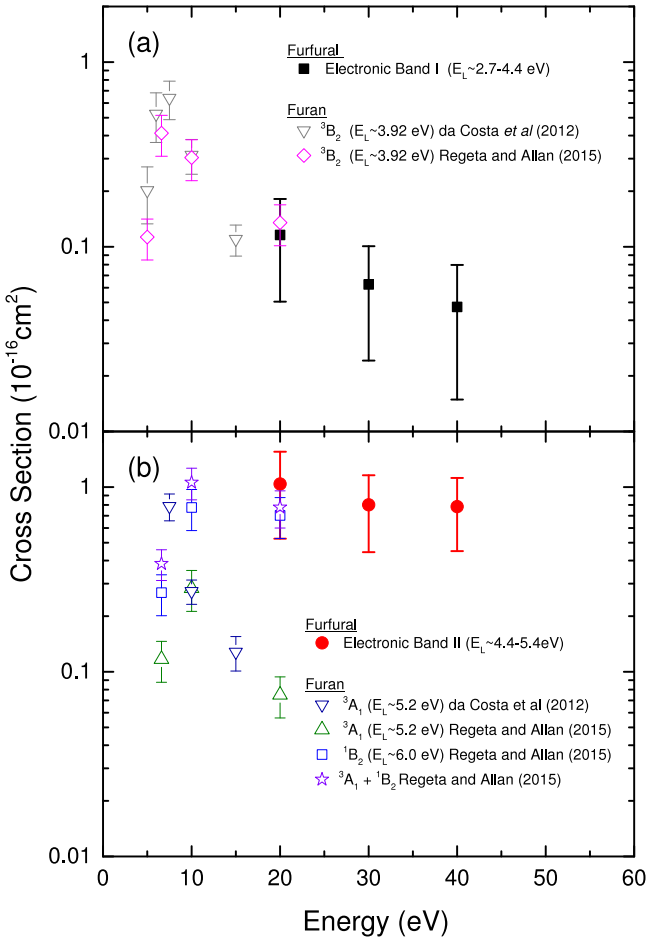

FIG. 2. Integral cross sections ($\times 10^{-16}$ cm^2) for electron impact excitation of (a) band I electronic-states and (b) band II electronic-states in furfural. Also shown are corresponding ICS for similar excitation processes in furan.[31,32] See legend in figure and text for further details.

oscillator strength (GOS) formalism[35,36] for optically allowed states, has also been described in some detail previously[37] and so again we do not repeat that detail here. The uncertainties on the present derived ICSs are also given in Table I and all are at the one standard deviation level. Those uncertainties arise from the intrinsic errors on the measured DCS and any uncertainty introduced through the interpolation/extrapolation of our data. The uncertainty limits on our ICS (see Table I) are found to be in the range 18%–69%, with the precise value depending on the E_0 and inelastic channel in question.

We have described our IAM-SCAR computations many times,[16,21–23,38] so that only a précis need be given here. In essence, an atomic optical potential scattering model calculates all the phase shifts for each of the atoms that comprise the species in question (i.e., carbon, oxygen, and hydrogen for furfural). The molecular scattering amplitudes then stem from the sum of all the relevant atomic amplitudes, including the phase coefficients. This is basically the so-called additivity rule (AR). However, the AR does not account for the target molecular structure, so that some screening coefficients (SCs) are also employed in order to account for the geometry of the molecule (atomic positions and bond lengths). Additionally, Blanco and García[27] recently introduced an interference term (I) to help describe that the collision dynamics involves scattering from multiple centres. Full details for this extension to the IAM-SCAR approach can be found in Ref. 27. Although we have previously plotted the elastic ICSs, as well as the total cross section, from this IAM-SCAR+I approach,[4,8] in Table II we list all the relevant data for the first time. It is interesting to compare the results from the IAM-SCAR+I and traditional IAM-SCAR approaches. The addition of the interference term in the calculation increases the elastic ICS by ~15% at 5 eV and up to 43% at 1000 eV. However, the interference term does not influence the total inelastic ICS. Note that in Table II, we also include rotational ICS from a Born-dipole approach and the total ionization cross sections from our BEB computation.[33,36] In the BEB approximation, the integral ionization cross section

TABLE II. Electron scattering cross sections ($\times 10^{-16}$ cm^2) obtained at the Born-dipole,[21–26] IAM-SCAR+I,[27] and BEB[33] levels for furfural. See text for further details.

Energy (eV)	Total IAM-SCAR+I	Elastic IAM-SCAR+I	Inelastic IAM-SCAR+I	Rotational (Born-dipole)	BEB-ionization
1	613.3	100.3		515.3	
1.5	442.4	83.2		358.4	
2	352.8	74.5		278.3	
3	260.7	66.6		194.1	
4	212.8	62.7		150.1	
5	182.9	60.2		122.7	
7	147.6	56.8	0.0	90.7	
10	119.6	53.8	0.1	65.5	0.0
15	98.0	49.3	3.3	45.4	1.0
20	86.8	43.7	8.2	35.0	3.0
30	74.5	37.0	13.6	24.2	6.7
40	66.9	33.3	15.3	18.6	9.0
50	61.0	30.2	15.7	15.1	10.3
70	53.2	26.3	15.7	11.1	11.5
75	51.5	25.6	15.5	10.4	11.6
100	45.6	22.7	14.8	8.0	11.6
150	37.8	18.9	13.2	5.5	10.7
200	32.5	16.4	11.9	4.2	9.7
250	28.8	14.6	10.8	3.4	8.8
300	26.1	13.3	9.9	2.9	8.0
400	22.0	11.2	8.5	2.2	6.8
500	19.1	9.8	7.5	1.8	5.9
700	15.3	7.8	6.1	1.3	4.7
1000	11.8	6.1	4.8	0.9	3.6

contributions from the i^{th} molecular orbital, Q_i, is obtained via

$$Q_i(t_i) = \frac{4\pi a_0^2 N_i (R/B_i)^2}{t_i + u_i + 1}\left[\frac{\ln(t_i)}{2}\left(1 - \frac{1}{t_i^2}\right) + 1 - \frac{1}{t_i} - \frac{\ln(t_i)}{t_i + 1}\right]. \tag{2}$$

In Eq. (2), $t_i = E_0/B_i$ and $u_i = U_i/B_i$, with a_0 and R being the Bohr radius and the Rydberg energy, respectively. N_i, B_i, and U_i are the ionized orbitals' occupation number, bound state binding energy, and average orbital kinetic energy, respectively. The present furfural average orbital kinetic energies were obtained from density functional theory (DFT), with a B3LYP/aug-cc-pVDZ model chemistry, calculations within the GAUSSIAN 09 code.[39] They were subsequently combined with experimental PES[5,28] and calculated OVGF/aug-cc-pVDZ (Ref. 5) ionization energies. The total ionization cross section, Q_{ion} (see Table II), is then obtained by summing up over the cross section contribution from the N-occupied furfural orbitals,

$$Q_{\text{ion}}(E_0) = \sum_{i=1}^{N} Q_i(t_i). \tag{3}$$

In the present study, we also employed the Schwinger multichannel method with pseudopotentials (SMCPP)[40–42] to obtain theoretical cross sections for the excitation of the previously discussed bands[4] of furfural by electron impact. This theory was recently reviewed in Ref. 41, and here we only give a brief summary of the working expressions relevant to the present work. In this method the scattering amplitude is given by

$$f(\mathbf{k}_f, \mathbf{k}_i) = -\frac{1}{2\pi}\sum_{m,n}\langle S_{\mathbf{k}_f}|V|\chi_m\rangle (d^{-1})_{mn}\langle\chi_n|V|S_{\mathbf{k}_i}\rangle, \tag{4}$$

where

$$d_{mn} = \langle\chi_m|\left[\frac{\hat{H}}{N+1} - \frac{\hat{H}P + P\hat{H}}{2} + \frac{PV + VP}{2} - VG_P^{(+)}V\right] \times |\chi_n\rangle. \tag{5}$$

In the Eqs. (4) and (5), P is a projector onto N_{open} energy-allowed target electronic channels, i.e.,

$$P = \sum_{\ell=1}^{N_{open}} |\,\Phi_\ell\rangle\langle\Phi_\ell\,|\,. \tag{6}$$

$G_P^{(+)}$ is the free-particle Green's function projected onto the P space, V is the interaction potential between the electron and the molecular target, $\mathbf{k}_i$ ($\mathbf{k}_f$) is the incoming (outgoing) electron wave vector, and $\hat{H} = E - H$ is the total collision energy minus the Hamiltonian of the $(N+1)$-electron system under the fixed nuclei approximation. Note that H is defined as $H = H_0 + V$, where H_0 represents the Hamiltonian for the non-interacting electron-molecule system and $S_{\mathbf{k}}$ is its corresponding solution, given by the product of a plane wave and a target state.

The $(N+1)$-electron trial basis, composed of configuration state functions (CSFs), denoted by χ_m, is built from anti-symmetrized products of target electronic states and single-particle (scattering) orbitals, with the proper spin-coupling. The open electronic collision channels are included in the P

space and the dynamical response of the target electrons to the projectile field (correlation-polarization effects) is accounted for through virtual excitations of the target. In this case, the CSFs are given by

$$|\chi_m\rangle = \mathcal{A}_{N+1}|\Phi_i(1,\ldots,N)\rangle \otimes |\varphi_j(N+1)\rangle, \tag{7}$$

where $|\Phi_i(1,\ldots,N)\rangle$ is a target state and $|\varphi_j(N+1)\rangle$ is a single-particle orbital which represents a scattering orbital.

The integral cross section (ICS) for the electronic excitation process $\Phi_n \rightarrow \Phi_{n'}$, where Φ_n denotes the target states, can be readily obtained from the scattering amplitude given in Eq. (4) by the following relation:

$$\sigma_{n\rightarrow n'}(E) = \frac{k_f}{k_i}\frac{1}{4\pi}\int d\hat{\mathbf{k}}_i \int d\hat{\mathbf{k}}_f\, |f(\mathbf{k}_f,\mathbf{k}_i)|^2. \tag{8}$$

In the expression above, the magnitude of the final wave vector is given by $k_f^2 = k_i^2 - 2(\epsilon'_n - \epsilon_n)$, where ϵ_n denotes the energy of the nth electronic target state. The integration over $\hat{\mathbf{k}}_f$ accounts for scattering into all the possible directions, while $(4\pi)^{-1}\int d\vec{k}_i$ averages over the random molecular orientations in the target gas. The integration over both the incoming and outgoing directions makes the ICS rotationally invariant and hence equal in both the molecule-fixed and laboratory-fixed reference frames. The ICSs for the bands considered in this work are simply obtained as a sum of the ICSs for each electronic excitation process involving the states that compose the specific band under consideration.[7]

In electron collisions with polar molecules or for dipole-allowed singlet transitions, we employ a Born-closure scheme to deal with the long range potential.[43] The scattering amplitude within the Born-closure is given by

$$\begin{aligned} f_{\mathrm{LAB}}^{\mathrm{closure}}(\mathbf{k}_f,\mathbf{k}_i) = {} & f_{\mathrm{LAB}}^{\mathrm{FBA}}(\mathbf{k}_f,\mathbf{k}_i) \\ & + \sum_{\ell=0}^{\ell_{max}}\sum_{m=-\ell}^{\ell}\left(f_{\mathrm{LAB}}(\ell m,\mathbf{k}_i) - f_{\mathrm{LAB}}^{\mathrm{FBA}}(\ell m,\mathbf{k}_i)\right) \\ & \times Y^*_{\ell m}(\mathbf{k}_f), \end{aligned} \tag{9}$$

where $f_{\mathrm{LAB}}^{\mathrm{FBA}}$ is the scattering amplitude for the permanent dipole moment potential for the elastic process or for the dipole transition potential for inelastic dipole-allowed processes. Both are obtained in the first Born approximation, in a closed form in the laboratory-frame, and the amplitude $f_{\mathrm{LAB}}(\ell m,\mathbf{k}_i)$ is just the $f(\ell m,\mathbf{k}_i)$ (which is the amplitude where $\mathbf{k}_f$ is expanded in partial waves) transformed to this frame.

The molecular geometry and the single-particle basis represented by Cartesian Gaussian functions, used in our calculations, are the same as reported by Ref. 8. As also discussed in that reference and in Jones *et al.*,[7] the minimum orbital basis for single-excitation configuration interaction (MOBSCI)[41] of the present application considered up to 31 triplet and 31 singlet electronic states (plus the ground electronic state), with 31 electronic states open at 10 eV (31ch-SEP approximation), 53 electronic states at 20 eV (53ch-SEP approximation), and all 63 electronic channels open at 30 and 40 eV (63ch-no additional closed channels for SEP). Note that the acronym SEP stands for static exchange plus polarisation.

III. RESULTS AND DISCUSSION

In Table I and Figure 1(a) we present, our experimental electron-impact ICSs for each of bands I–VI in furfural, and the ICS for the sum of these electronic-state bands. The energy range of those experiments is 20–250 eV. Note, however, the energy resolution of the measurements at 250 eV was poorer than those between 20 and 40 eV,[7] so that at 250 eV, ICSs are only reported for bands I + II + III and bands IV + V + VI and their sum. Further note that as band I is comprised of two triplet states and a symmetry-forbidden singlet state,[4,7] its contribution at 250 eV will be minimal so that the ICS here, for all intents and purposes, essentially corresponds to that for bands II + III. It is clear from Fig. 1(a) that the smallest magnitude ICS corresponds to excitation of band I, while the largest magnitude ICS corresponds to that for excitation of band II. This observation is entirely consistent with the energy loss spectra previously reported in the work of Jones *et al.*,[7] and with the fact that the strongest dipole-allowed electronic-state excitation in furfural (to a ^{1}A′ state at $E_{\mathrm{L}} \sim 4.79$ eV) lies in band II.[4] With the exception of band I, where the magnitude of its ICS dies off quite quickly as E_0 is increased from threshold (consistent with its spectroscopy as noted above[4]), the energy dependence of the ICSs for bands II–VI are all quite similar (see Fig. 1(a)). We believe this observation is consistent with the discrete electronic-state spectroscopy of furfural, as discussed by Ferreira da Silva *et al.*,[4] as each of bands II–VI largely consists of a mixture of triplet, symmetry-forbidden singlet, dipole-allowed singlet, and Rydberg states.

Finally, for bands I and II, we can compare the measured ICS to corresponding results from our SMCPP computations. Excellent qualitative (i.e., the shape of the ICS as a function of energy) accord is found for both bands, with the reasons for the mismatch in absolute value having been described in detail previously.[7] Briefly, however, the magnitude discrepancy is thought to be due to the finite size of our present MOBSCI and that coupling to the continuum is currently not considered.

Also plotted in Fig. 1(a) are the results of our total ionization cross section (TICS) calculation using a BEB approach,[33,36] and our total inelastic ICS (except for vibrational excitation) from our current IAM-SCAR+I computation. If we now add the sum of our electronic-state ICSs to the sum of the vibrational ICSs from Jones *et al.*[6] and our TICS, then that might be compared to the IAM-SCAR+I total inelastic ICS. We note that we are not strictly comparing "apples with apples" in this case, as the former sum does not include an ICS for neutral dissociation while the IAM-SCAR+I result ignores vibrational excitation. Nonetheless, as we glean from Fig. 1(a), the agreement between them is really quite excellent and provides a nice self-consistency check for those results. This gives us some confidence that a furfural cross section data base might also be assembled for plasma modelling studies.

In Fig. 1(b), we again plot the experimental ICS sums for electronic-state and vibrational excitation,[6] and our BEB results[33,36] and the sum of all these component cross sections, but now we compare them to our IAM-SCAR+I results for the total cross section (TCS), rotational ICS, elastic ICS and, as before, the total inelastic ICS. Note that all our

IAM-SCAR+I theory results are summarised in Table II. The main point of this figure is to graphically illustrate just what a small contribution to the TCS that discrete electronic-state excitation actually makes. Indeed its contribution to the TCS increases from only ~2.9% at 20 eV to ~8.4% at 250 eV, with ionization clearly being the dominant inelastic process above about 20 eV. Nonetheless, as has been explicitly demonstrated by White and colleagues on several occasions,[9,10] while the discrete electronic-state cross sections may be relatively small for a given molecule, they cannot be ignored if one wishes to provide a quantitative description for electron transport in gas discharges.

Let us now consider Figure 2, where we compare our band I and band II furfural ICSs, respectively, to corresponding electronic-state ICSs in furan from the work of da Costa *et al.*[31] and Regeta and Allan.[32] Specifically, in Fig. 2(a), we compare the present band I results to those for the furan $^3B_2$ state,[31,32] while in Fig. 2(b), we compare our band II ICS results to those for the ($^3A_1 + {}^1B_2$) states in furan.[31,32] While it is true that the current furfural and previous furan results only explicitly overlap at $E_0 = 20$ eV, we can still also look at the trends in the energy dependence of both sets of data. It is apparent from Fig. 2(a) that the relevant furfural (band I) and furan ($^3B_2$)[32] electronic-state ICSs are in excellent agreement at 20 eV, and that the trends in the energy dependence of both sets of ICS are also in very good accord. Similarly, for the band II ICSs of furfural and ($^3A_1 + {}^1B_2$) ICSs in furan, very good agreement between our results and those of Regeta and Allan[32] is found at 20 eV and in the energy trends of both sets of data (see Fig. 2(b)). The exciting prospect from the results embodied in Figs. 2(a) and 2(b) is that we might use the furan results from Regeta and Allan to extend our furfural results to lower energies and thereby further complete our furfural cross section data base for gas discharge and/or plasma modelling simulations. Of course it would be much better if the actual furfural data were available, but in its absence our suggestion, undertaken with appropriate caution, is undoubtedly superior to having no lower energy ICSs at all. Finally, for band I in furfural and the $^3B_2$ state in furan, we note that we also find a satisfactory level of accord between our results and those of da Costa *et al.*[31]

IV. CONCLUSIONS

We have reported on a series of integral cross section results, for electron impact excitation ($E_0 = 20$–250 eV) of bands of electronic-states in furfural. Those experimentally derived ICSs were supplemented with calculations using our IAM-SCAR+I model, our SMCPP model, and also a BEB model for the total ionization cross sections. Where a comparison between measurements and theory could be made, very good quantitative (but in some cases only qualitative) agreement was typically found. Similarly, when a comparison was made between our furfural band I and band II electronic-state ICSs, with corresponding furan electronic-state results from Regeta and Allan,[32] rather good accord was also found. As one of the aims of this study was to provide absolute cross sections that could be incorporated into simulations of atmospheric-plasma action on biomass, we consider the present investigation to have been successful to some degree. Further work, however, even though furfural is not a particularly nice species to work with experimentally,[6,7] is needed to push the available measurements closer to threshold. Nonetheless, if the present results were combined with our earlier work on elastic cross sections (including the momentum transfer cross section),[8] vibrational excitation cross sections,[6] and ionization,[5] then a reasonable database starting point, for simulations where furfural is a constituent, has probably been achieved.

ACKNOWLEDGMENTS

D.B.J. thanks the Australian Research Council (ARC) for financial support provided through a Discovery Early Career Research Award, while M.J.B. also thanks the ARC for their support. M.J.B. acknowledges the Brazilian agency CNPq for his "Special Visiting Professor" position at the Federal University of Juiz de Fora. G.G. acknowledges partial financial support from the Spanish Ministry MINECO (Project No. FIS2012-31230) and the European Union COST Action No. CM1301 (CELINA). Finally R.F.C., M.T.doN.V, M.H.F.B, and M.A.P.L. also acknowledge support from CNPq, while M.T.doN.V. thanks FAPESP.

[1]A. S. Mamman, J.-M. Lee, Y.-C. Kim, I. T. Hwang, N.-J. Park, Y. K. Hwang, J.-S. Chang, and J.-S. Hwang, Biofuels, Bioprod. Biorefin. **2**, 438 (2008).
[2]J. Amorim, C. Oliveira, J. A. Souza-Corrêa, and M. A. Ridenti, Plasma Processes Polym. **10**, 670 (2013).
[3]N. Schultz-Jensen, F. Leipold, H. Bindslev, and A. Thomsen, Appl. Biochem. Biotechnol. **163**, 558 (2011).
[4]F. Ferreira da Silva, E. Lange, P. Limão-Vieira, N. C. Jones, S. V. Hoffmann, M.-J. Hubin-Franskin, J. Delwiche, M. J. Brunger, R. F. C. Neves, M. C. A. Lopes, E. M. de Oliveira, R. F. da Costa, M. T. do N. Varella, M. H. F. Bettega, F. Blanco, G. García, M. A. P. Lima, and D. B. Jones, J. Chem. Phys. **143**, 144308 (2015).
[5]D. B. Jones, E. Ali, K. L. Nixon, P. Limão-Vieira, M.-J. Hubin-Franskin, J. Delwiche, C. G. Ning, J. Colgan, A. J. Murray, D. H. Madison, and M. J. Brunger, J. Chem. Phys. **143**, 184310 (2015).
[6]D. B. Jones, R. F. C. Neves, M. C. A. Lopes, R. F. da Costa, M. T. do N. Varella, M. H. F. Bettega, M. A. P. Lima, G. García, F. Blanco, and M. J. Brunger, J. Chem. Phys. **143**, 224304 (2015).
[7]D. B. Jones, R. F. C. Neves, M. C. A. Lopes, R. F. da Costa, M. T. do N. Varella, M. H. F. Bettega, M. A. P. Lima, G. García, P. Limão-Vieira, and M. J. Brunger, J. Chem. Phys. **144**, 124309 (2016).
[8]R. F. da Costa, M. T. do N. Varella, M. H. F. Bettega, R. F. C. Neves, M. C. A. Lopes, F. Blanco, G. García, D. B. Jones, M. J. Brunger, and M. A. P. Lima, J. Chem. Phys. **144**, 124310 (2016).
[9]K. F. Ness, R. E. Robson, M. J. Brunger, and R. D. White, J. Chem. Phys. **136**, 024318 (2012).
[10]J. de Urquijo, E. Basurto, A. M. Juárez, K. F. Ness, R. E. Robson, M. J. Brunger, and R. D. White, J. Chem. Phys. **141**, 014308 (2014).
[11]A. G. Sanz, M. C. Fuss, A. Muñoz, F. Blanco, P. Limão-Vieira, M. J. Brunger, S. J. Buckman, and G. García, Int. J. Radiat. Biol. **88**, 71 (2012).
[12]R. D. White, W. Tattersall, G. Boyle, R. E. Robson, S. Dujko, Z. Lj. Petrovic, A. Bankovic, M. J. Brunger, J. P. Sullivan, S. J. Buckman, and G. García, Appl. Radiat. Isot. **83**, 77 (2014).
[13]A. Muñoz, F. Blanco, G. García, P. A. Thorn, M. J. Brunger, J. P. Sullivan, and S. J. Buckman, Int. J. Mass Spectrom. **277**, 175 (2008).
[14]M. C. Fuss, L. Ellis-Gibbings, D. B. Jones, M. J. Brunger, F. Blanco, A. Muñoz, P. Limão-Vieira, and G. García, J. Appl. Phys. **117**, 214701 (2015).
[15]G. B. da Silva, R. F. C. Neves, L. Chiari, D. B. Jones, E. Ali, D. H. Madison, C. G. Ning, K. L. Nixon, M. C. A. Lopes, and M. J. Brunger, J. Chem. Phys. **141**, 124307 (2014).
[16]R. F. da Costa, E. M. de Oliveira, M. H. F. Bettega, M. T. do N. Varella, D. B. Jones, M. J. Brunger, F. Blanco, R. Colmenares, P. Limão-Vieira, G. García, and M. A. P. Lima, J. Chem. Phys. **142**, 104304 (2015).

[17]R. F. C. Neves, D. B. Jones, M. C. A. Lopes, K. L. Nixon, E. M. de Oliveira, R. F. da Costa, M. T. do N. Varella, M. H. F. Bettega, M. A. P. Lima, G. B. da Silva, and M. J. Brunger, J. Chem. Phys. **142**, 194302 (2015).
[18]R. F. C. Neves, D. B. Jones, M. C. A. Lopes, K. L. Nixon, G. B. da Silva, H. V. Duque, E. M. de Oliveira, R. F. da Costa, M. T. do N. Varella, M. H. F. Bettega, M. A. P. Lima, K. Ratnavelu, G. García, and M. J. Brunger, J. Chem. Phys. **142**, 104305 (2015).
[19]D. B. Jones, G. B. da Silva, R. F. C. Neves, H. V. Duque, L. Chiari, E. M. de Oliveira, M. C. A. Lopes, R. F. da Costa, M. T. do N. Varella, M. H. F. Bettega, M. A. P. Lima, and M. J. Brunger, J. Chem. Phys **141**, 074314 (2014).
[20]R. F. C. Neves, D. B. Jones, M. C. A. Lopes, F. Blanco, G. García, K. Ratnavelu, and M. J. Brunger, J. Chem. Phys. **142**, 194305 (2015).
[21]M. C. Fuss, A. G. Sanz, F. Blanco, J. C. Oller, P. Limão-Vieira, M. J. Brunger, and G. García, Phys. Rev. A **88**, 042702 (2013).
[22]A. G. Sanz, M. C. Fuss, F. Blanco, J. D. Gorfinkiel, D. Almeida, F. Ferreira da Silva, P. Limão-Vieira, M. J. Brunger, and G. García, J. Chem. Phys. **139**, 184310 (2013).
[23]H. Kato, A. Suga, M. Hoshino, F. Blanco, G. García, P. Limão-Vieira, M. J. Brunger, and H. Tanaka, J. Chem. Phys. **136**, 134313 (2012).
[24]J. R. Brunton, L. R. Hargreaves, S. J. Buckman, G. García, F. Blanco, O. Zatsarinny, K. Bartschat, and M. J. Brunger, Chem. Phys. Lett. **568-569**, 55 (2013).
[25]J. R. Brunton, L. R. Hargreaves, T. M. Maddern, S. J. Buckman, G. García, F. Blanco, O. Zatsarinny, K. Bartschat, D. B. Jones, G. B. da Silva, and M. J. Brunger, J. Phys. B **46**, 245203 (2013).
[26]P. Palihawadana, J. P. Sullivan, S. J. Buckman, Z. Mašín, J. D. Gorfinkiel, F. Blanco, G. García, and M. J. Brunger, J. Chem. Phys. **139**, 014308 (2013).
[27]F. Blanco and G. García, Chem. Phys. Lett. **635**, 321 (2015).
[28]D. Klapsein, C. D. MacPherson, and R. T. O'Brien, Can. J. Chem. **68**, 747 (1990).
[29]A. R. Smith and G. Meloni, J. Mass Spectrom. **50**, 1206 (2015).
[30]M. H. Palmer, I. C. Walker, C. C. Ballard, and M. F. Guest, Chem. Phys. **192**, 111 (1995).
[31]R. F. da Costa, M. H. F. Bettega, M. A. P. Lima, M. C. A. Lopes, L. R. Hargreaves, G. Serna, and M. A. Khakoo, Phys. Rev. A **85**, 062706 (2012).
[32]K. Regeta and M. Allan, Phys. Rev. A **91**, 012707 (2015).
[33]Y.-K. Kim and M. E. Rudd, Phys. Rev. A **50**, 3954 (1994).
[34]M. J. Brunger and P. J. O. Teubner, Phys. Rev. A **41**, 1413 (1990).
[35]E. N. Lassettre, J. Chem. Phys. **43**, 4479 (1965).
[36]H. Tanaka, M. J. Brunger, L. Campbell, H. Kato, M. Hoshino, and A. R. P. Rau, "Scaled plane-wave Born cross sections for atoms and molecules," Rev. Mod. Phys. (in press).
[37]Z. Mašín, J. D. Gorfinkiel, D. B. Jones, S. M. Bellm, and M. J. Brunger, J. Chem. Phys. **136**, 144310 (2012).
[38]L. Chiari, H. V. Duque, D. B. Jones, P. A. Thorn, Z. Pettifer, G. B. da Silva, P. Limão-Vieira, D. Duflot, M.-J. Hubin-Franskin, J. Delwiche, F. Blanco, G. García, M. C. A. Lopes, K. Ratnavelu, R. D. White, and M. J. Brunger, J. Chem. Phys. **141**, 024301 (2014).
[39]M. J. Frisch *et al.*, GAUSSIAN 09, Revision B.01, Gaussian, Inc., Wallingford, CT, USA, 2010.
[40]M. H. F. Bettega, L. G. Ferreira, and M. A. P. Lima, Phys. Rev. A **47**, 1111 (1993).
[41]R. F. da Costa, F. J. da Paixão, and M. A. P. Lima, J. Phys. B **37**, L129 (2004).
[42]J. S. dos Santos, R. F. da Costa, and M. T. do N. Varella, J. Chem. Phys. **136**, 084307 (2012).
[43]R. F. da Costa, M. T. do N. Varella, M. H. F. Bettega, and M. A. P. Lima, Eur. Phys. J. D **69**, 159 (2015).